Water Practice & Technology Vol 14 No 2
doi: 10.2166/wpt.2019.014

Nanofibers for textile waste water management

Joginder singh Paneysar[a], Snehal Sawant[a], Meng Hei Ip[b], Sukhwinder kaur Bhullar[c,d], Stephen Barton[b], Premlata Ambre[a,*] and Evans Coutinho[a]

[a] Department of Pharmaceutical Chemistry, Bombay College of Pharmacy, Mumbai 400 098, India

[b] School of Life Sciences, Pharmacy and Chemistry, Kingston University, Kingston-upon-Thames KT1 2EE, UK

[c] Department of Mechanical Engineering, Bursa Technical University, Bursa 16190, Turkey

[d] Present address: St. Boniface Hospital, Albrechtsen Research Centre, Winnipeg, MB, Canada

*Corresponding author. E-mail: premlata.ambre@bcp.edu.in

Abstract

Currently, textile wastewater management focuses on dye removal efficiency and operating costs. Dual responsive polymers are choice materials because they can extract diverse organic compounds from water at their phase transition point. They are copolymers of the acrylamide class, and have been fully characterized by FT-IR, ^{1}H-NMR, DSC, GPC and surface area analysis. Of the five dual responsive polymers, the copolymer of NIPAAM and DMAEMA (CoP-1) offers the best extraction of acidic and basic dyes from wastewater. All copolymers investigated can achieve better than 90% dye removal when used at 4 mg/ml concentration. This dye-scavenging efficiency increases to almost 99% at 3 mg/ml, on conversion of the copolymers to nanofibers in 300 to 500 nm size. Langmuir and Freundlich isotherms were constructed to study the mechanism of dye adsorption. The nanofibers have been shown to be reusable for removal of dyes from water, suggesting that such systems may add benefit to current dye removal methods from textile industry wastewater.

Key words: adsorption isotherm, dual responsive polymers, smart nanofibers, textile dyes, textile water management

INTRODUCTION

Water shortages and stringent regulatory strictures in recent years have encouraged the development of novel systems for water reuse. Providing potable water at a rate to match increase in population with decrease in water quality, available resources and climate change is a great challenge (Robinson *et al.* 2001). The textile industry is a prime culprit in water pollution, posing risk to human and aquatic life. The industry produces around 80 million tonnes of fibers per year (mt/a) and total dye consumption for these fibers exceeds 1 mt/a. Textile dye concentrations are usually between 10 and 200 mg/L, and about 10 to 15% of the dye is lost in the process (Liang *et al.* 2014). Further processing, including washing, releases more dye, which is drained as effluent. These dyes increase the turbidity of water, and make it look and smell bad, additionally inhibiting the penetration of sunlight necessary for photosynthesis. Dissolved oxygen is essential for life in water and its depletion is the most serious effect of textile waste discharge, which also hinders natural purification processes.

Stringent laws have been proposed that limit the amounts and kinds of waste that can be released as effluent. The extensive release of textile dyes with adverse effects on the environment and public health, means that serious efforts are required to reduce pollution. This can be achieved using efficient effluent treatment systems at textile industry sites. Various methods have been devised for treatment

Water Practice & Technology Vol 14 No 2
doi: 10.2166/wpt.2019.014

of dye wastewaters which can be broadly classified as physical, chemical and/or biological, depending on the application. Physical methods include adsorption, membrane filtration, irradiation, coagulation, reverse osmosis, ultra-filtration and nanofiltration. Of all these technologies, adsorption is the simplest and is effective as it offers high removal efficiency for a wide spectrum of dye-types (Elmoubarki *et al.* 2015). No additional materials are needed to operate these processes, thereby offering high efficiency, and helping to preserve available water resources by both increased efficiency and ease of operation.

Nanotechnology is used in adsorption in various forms like nanoparticles, nanotubes and nanofibers, and has the potential to remove metal ions, dyes, and various organic and inorganic species. In particular, polymeric nanofibers have become popular in the past few years for removal of contaminants from water. The non-woven material produced by electrospinning has several attractive features including a diameter below 500 nm, large surface area, high porosity, high gas permeability and small pore size. Swaminathan *et al.* (2015) report on use of an electrospun nanofibrous composite mat prepared from polyacrylonitrile (PAN) yarn waste and graphene oxide for removal of methylene blue from water. Electrospun polyvinylalcohol/titanium oxide (PVA)/TiO_2 composite membranes followed by photocatalysis have also been reported to remove methylene blue from water (Ismaya *et al.* 2017). Chen *et al.* (2016) report dye removal using cellulose-based graphene oxide fibres, demonstrating the extensive capability of polymers.

Dual responsive polymers are a class of materials that exhibit different properties at different temperature and pH ranges. Dual responsive polymeric microgel-based assemblies have already established efficiency for removal of organic dyes from water (Parasuraman & Serpe 2011). With respect to temperature response, these polymers are soluble in water at room temperature but precipitate at higher temperatures. Likewise, pH responsive polymers are completely soluble in water over a certain pH range but precipitate just outside it. The transition point from soluble to insoluble, triggered by temperature or pH, is termed the cloud point (CP) and defined as the first appearance of turbidity for a clear polymeric solution. Lower critical solution temperature (LCST) is used in relation to temperature responsive polymers and is the point above which the polymer chains start orienting themselves in such a manner that hydrogen bonding efficiency is reduced, and the chains become hydrophobic. This hydrophobic state is responsible for the adsorption of most organic contaminants from water (Paneysar *et al.* 2017). The temperature responsive polymers include the acrylamide class – e.g., poly(N-isopropylacrylamide) (PNIPAAM), poly(N,N-diethylacrylamide) (PNNDEA), poly(N-vinylcaprolactum) (PNVCL), poly(N-vinyl isobutyramide) (PNVIB), etc – whereas the pH responsive polymers include polyvinylpyrrolidone (PVP), polyacrylic acid (PAA), polymethacrylic acid (PMA), polyethylacrylic acid (PEA), poly propylacrylic acid (PPA), etc. The monomers from the two categories, when copolymerized, yield polymers that respond to both temperature and pH at the phase transition point (Liang *et al.* 2015), and are classified as dual responsive polymers. They include poly dimethylaminoethyl methacrylate (PDMAEMA) and poly diethylaminoethyl methacrylate (PDEAEMA), both available commercially. Dual responsive polymers have reportedly been used for peptide (Aguilar *et al.* 2007), DNA (Hinrichs *et al.* 1999), transdermal (Samah & Heard 2013), and drug delivery systems (Zheng *et al.* 2017) for anticancer therapy (Zhu *et al.* 2010), as well as dye removal from wastewater (Marques *et al.* 2015).

This study focuses on the development of dual responsive polymers and evaluation of their application in textile wastewater treatment. Water discharged by the textile industry is usually at higher than ambient temperature and with varied pH, so the properties of dual responsive polymers could be appropriate under these conditions. These polymers and their nano-fabricated products – nanofibers – were evaluated in the study. Since textile wastewater has dyes as the primary component, the aim was their removal with maximum efficiency.

Water Practice & Technology Vol 14 No 2
doi: 10.2166/wpt.2019.014

MATERIALS AND METHODS

Materials

The monomer N-isopropylacrylamide (NIPAAM) was obtained as a gift sample from SLN Pharma chem (Mumbai, India), and dimethylaminoethyl methacrylate (DMAEMA) was a gift sample from Ess Emm chemicals (Mumbai, India), diethylacrylamide (DEA) was procured from TCI chemicals (Chennai, India) and vinylpyrolidone (VP) from Sigma-Aldrich (Mumbai, India). The free radical initiator azobisisobutyronitrile (AIBN) was purchased from Spectrochem Pvt. Ltd (Mumbai, India) and dialysis membrane from HiMedia (Mumbai, India).

Methods

Synthesis of smart dual responsive polymers

The monomers were combined and dissolved in 5 ml ethanol in different weights and ratios – see Table 1. The initiator (AIBN) was added under a nitrogen atmosphere and the reaction was carried out at 70 °C to initiate polymerization. The ethanol in the medium was removed under vacuum using a rotary evaporator, after which the viscous solution was poured into hexane and the precipitate dissolved in ethyl acetate. This was repeated two or three times to remove starting materials and reactants, and the crude copolymer was dried under vacuum. The copolymer was purified by dialysis against distilled water for three days in a membrane with a molecular weight cut-off of 12,000 to 14,000 Da. After dialysis the solutions were lyophilized, giving free-flowing powders. Table 1 gives details of the monomer and agent ratios used for copolymerization, and Figure 1 shows the general copolymerization scheme.

Table 1 | Quantities of reactants and time taken for copolymerization, and respective polymer cloud points

		Monomers								Cloud
Code	Copolymer	NIPAAM	DEA	VP	DMAEMA	Initiator (AIBN)	Solvent (Ethanol)	Time (Hrs.)	LCST (°C)	point (pH)
CoP-1	NIPAAM-DMAEMA (14:1)	1.1 gm (10 mmol)	–	–	118 µl (0.7 mmol)	10 mg	5 ml	24	37	10.0
CoP-2	DEA-DMAEMA (1:14)	–	700 µl (5.76 mmol)	–	60 µl (0.41 mmol)	10 mg	5 ml	10	28	9.5
CoP-3	NIPAAM-VP (1:1.5)	0.425 gm (3.86 mmol)	–	0.55 ml (5.1 mmol)	–	10 mg	5 ml	09	30	12.0
CoP-4	DEA-VP (10:1)	–	700 µl (5.76 mmol)	60 µl (0.56 mmol)	–	10 mg	5 ml	24	45	10.5
CoP-5	DMAEMA-VP (5:1)	–	–	770 µl (6.55 mmol)	210 µl (1.27 mmol)	10 mg	5 ml	4	50	9.0

Electrospinning

CoP-1 (0.6 gm); CoP-2 (0.15 gm); CoP-4 (0.7 gm) and undiluted polycaprolactone (PCL) (0.8 gm) were individually dissolved in chloroform to obtain a 10% w/v polymer solution for fabrication of nanofibers NF-1, NF- 2, NF- 4 and PCL respectively. Electrospinning was carried out at 30 kV and 0.25 ml/min flow rate, using an Inovenso Nanospinner24. Nanofibers were collected on a drum covered with aluminium foil rotating at 100 rpm. The collector/needle distance was 10 cm and 10 ml of solution was used completely for each sample to spin the same amount of fiber each time. The nanofibers were dried in a fume hood for 24 hours at room temperature.

Water Practice & Technology Vol 14 No 2
doi: 10.2166/wpt.2019.014

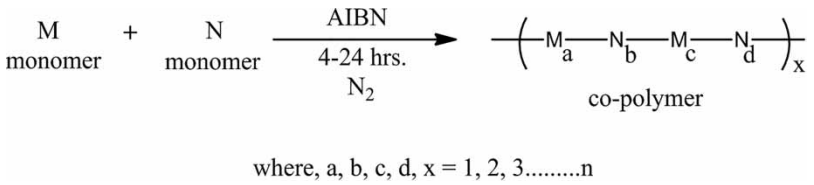

Figure 1 | General copolymerization scheme.

Determination of CP/LCST of the copolymer under the influence of temperature and pH

LCST was determined by the cloud point method – visual examination – by increasing the temperature linearly of a 2.5% solution of copolymer from 20 to 40 °C. The temperature at which the solution turned turbid was noted as the CP (the temperature at which the polymer precipitated), and expressed as the LCST. The CP was confirmed using a Mettler (Toledo) DSC 822e unit. Similarly, the pH of the polymer solutions was varied from 2 to 13 and the point of first appearance of turbidity was noted.

FT-IR analysis

Potassium bromide (KBr) discs with the copolymers were prepared using an electrically operated Techno Search Instruments KBr press model HP-15 (Mumbai, India). IR spectra were recorded on a Jasco FTIR-5300 Fourier transform spectrophotometer with a resolution of 4 cm^{-1}.

^{1}H-NMR characterization

NMR spectra of the copolymers were recorded using a Brüker Avance III 800 MHz FT-NMR spectrometer. The NMR samples were each made in solution comprising 0.9 ml H_2O and 0.1 ml D_2O.

Molecular weight determination

Gel permeation chromatography

Gel permeation chromatography (GPC) was performed with a Varian Pro Star 210 solvent delivery module and a Phenomonex Yarra 3u SEC-4000 aqueous GPC column (column size 300 × 7.8 mm). Data collection was driven by Galaxie Chromatography Software; 100 mM Na_2HPO_4 buffer (pH 6.8) was used as the mobile phase at a constant flow rate of 1 ml/min. All polymer samples were detected by UV at 280 nm. GPC standards were used to calibrate the instrument prior to sample analysis. Twenty μl of the calibration standard solution (protein mixture and uridine) was injected in each case and the analysis run for 20 minutes.

Surface area determination

Brunauer-Emmett-Teller (BET) surface area analysis and Barrett-Joyner-Halenda (BJH) pore size and volume analysis were performed on a Belsorp Mini II (Metrohm). Nitrogen adsorption and desorption by the polymer were studied. The measuring range of the instrument for surface area was 0.01 m^2/g and pore size 0.35 to 200 nm. A weighed sample was loaded into a glass tube and, as pre-treatment, was degassed for three hours at 110 °C and 10^{-2} kPa pressure. The sample was then rechecked to obtain the actual weight and the sample cell (glass tube) loaded into the instrument for analysis.

Water Practice & Technology Vol 14 No 2
doi: 10.2166/wpt.2019.014

Nanofiber characterization

The surface morphology of the nanofibers was studied by scanning electron microscopy (SEM). The average nanofiber diameter was measured from images captured with a ZEISS EVO 40 microscope and sputter-coating was done with BAL-TEC SCD 005. The samples were prepared on a base coating of gold-palladium (60% : 40%) to make them appropriate for electron sample interaction. The sample was coated for 100 to 200 seconds to a thickness between 5 and 30 nm. After coating, the samples were kept in the SEM chamber and the system was subjected to high vacuum while imaging.

Evaluation and optimization of adsorption potential

Dyes are released daily as effluents by the textile industry, and may be classified as acidic, basic, direct, mordant, vat, reactive, disperse, azo and/or sulphur dyes. Methylene blue and crystal violet were selected as representative basic dyes, whereas Congo red, methyl orange, and indigo carmine were selected to represent acidic dye species for the study. The proportional dye removal by the copolymers was evaluated by UV-visible spectroscopy.

A fixed concentration of each dye with absorbance within the linear range of the Beer-Lambert law was selected, and the solutions treated with the copolymers and nanofibers. The conditions for adsorption were optimised by varying the copolymer concentration and the contact time above the respective CPs. Two copolymer concentrations, 1 and 4 mg/ml, were added to the dye solution and heated above the CP for various times. The solutions were then filtered, the precipitate removed and the absorbance of the final solution measured by UV. The proportional dye removal was calculated using Equation (1):

$$\text{proportional} \quad \text{dye removal} = \frac{Co - Ce}{Co} \times 100 \tag{1}$$

where, Co: dye concentration before treatment, and Ce: dye concentration after equilibrium and treatment.

All the proportional removal or adsorption analysis studies were performed in triplicate.

Adsorption parameter optimization

The copolymers are highly soluble in water and precipitate only above the cloud point (CP). Precipitation is caused by transformation of the copolymer into hydrophobic coiled chains that are responsible for absorption of the dye. To determine the polymers' maximum adsorption ability initially, a low concentration (1 mg/ml) of copolymer was added to a solution containing a fixed concentration of dye (methylene blue – 3 mg/L). The solution temperature and pH were increased steadily, and then kept constant above the individual polymers' CPs for a range of times. The proportional adsorption was calculated for various times to determine the maximum dye adsorption. In a second study, the polymer concentration was kept at 4 mg/ml and the adsorption time for equilibrium determined.

Since, the adsorption of impurities depends largely on the polymer's specific surface area, it was decided to test the polymers' power when fabricated as nanofibers. Different weights of nanofibers were used for removal of dye from water above the LCST and pH responsive CP. The difference between the UV-visible absorbance of the dye solution before (inlet) and after (outlet) passing through the nanofibers was calculated to determine the amount of dye adsorbed. Since all nanofibers were blended with PCL for fabrication, blank PCL nanofibers were also evaluated for removal of dye from water.

Water Practice & Technology Vol 14 No 2
doi: 10.2166/wpt.2019.014

Optimization of adsorption potential using nanofibers

Between 5 and 50 mg of nanofibers were taken, in 5 mg intervals, and tested for dye removal. Proportional removal of dye was at a maximum with 30 mg of nanofiber (3 mg/ml) for 10 ml methylene blue solution (3 mg/L), and this concentration was then fixed with the optimised contact time at respective temperature and pH to evaluate removal by nanofibers. Similarly, adsorption by PCL nanofibers was also studied at the same concentration and it was found that these 'blank' nanofibers could also adsorb dyes from water.

Determination of particle size of copolymer at CP

To measure the particle size at LCST and CP, copolymer CoP-1 was dissolved in water to prepare two solutions each of 2.5% concentration. The temperature and pH of the solutions were increased slowly, and the particle size beyond the CP was measured with a Malvern Zetasizer Nano ZS.

Adsorption isotherm determination (Akl & Abou-Elanwar 2015)

Sorption isotherm studies were used to determine and explain the relationship between *Ceq*, the equilibrium concentration of the adsorbate (the copolymers), and the amount adsorbed at the surface. The Langmuir and Freundlich isotherm models were used to analyse the copolymers above their CPs at the optimised temperatures, pHs and contact times.

Langmuir adsorption isotherm

The Langmuir model exhibits a linear relationship for the amount of dye adsorbed per unit mass of adsorbent copolymer. It is distinguished by three factors – adsorption, desorption and kinetic rates – combined with the total number of free sites available on the surface. The collective surface concentration of dye is denoted by q.

Equation (2) is the linear form of the Langmuir equation:

$$\frac{C_e}{q_e} = \frac{1}{q_m K_L} + \frac{C_e}{q_m} \tag{2}$$

where, q_e (mg/g) is the amount of dye adsorbed per unit mass of copolymer (sorbent), C_e (mg/l) the final concentration of unadsorbed dye in solution, q_m (mg/g) the monolayer adsorption capacity and K_L (l/mg) the Langmuir equilibrium constant.

q_e is expressed as,

$$q_e = \frac{(C_i - C_f)V}{\text{mass}} \tag{3}$$

where, C_i is the initial concentration, C_f the final concentration, and V the volume of dye solution. The volume of dye and mass of polymer remain constant for a given set of analyses.

A graph of C_e/q_e against C_e gives the Langmuir isotherm.

Freundlich adsorption isotherm

This isotherm was developed using the assumption that the adsorbent has a heterogeneous surface with numerous adsorption sites.

Water Practice & Technology Vol 14 No 2
doi: 10.2166/wpt.2019.014

The linear form of the Freundlich Equation is (4):

$$q_e = K_f C_e^{\frac{1}{n}} \tag{4}$$

where n is the Freundlich exponent and K_f the Freundlich constant, which measures heterogeneity; the higher K_f, the more heterogeneous the adsorbent. To determine the Freundlich isotherm a plot of log q_e against log C_e gives a slope equal to 1/n and an intercept at logK_f. The slope 1/n represents a collective value of the relative magnitude of adsorption intensity for a certain sorption process.

$$\log q_e = \log K_f + \frac{1}{n} \log C_e \tag{5}$$

To determine the applicability and suitability of a specific isotherm model to the experimental data, regression coefficient (R^2) values were calculated from the plot of log q_e v/s log k_f. Comparison of the two models is based on the value of R^2. The Langmuir constants are obtained from the slope (q_m) and intercept (K_L), and the model's characteristics can be expressed in terms of R_L, a dimensionless constant for the separation factor to depict whether the adsorption is favourable or unfavourable – Equation (6):

$$R_L = \frac{1}{1 + K_L C_i} \tag{6}$$

where, C_i is initial concentration. The characteristics of R_L for favourable adsorption are $0 < R_L < 1$, for unfavourable adsorption $R_L > 1$, for linear adsorption $R_L = 1$, and for irreversible adsorption $R_L = 0$.

Reusability of nanofibers

The reusability was determined by measuring the number of times an optimised weight of nanofiber could be used to lower dye concentration from a fresh solution to 50% of its initial value, each time. To do this the optimised weight of nanofiber was added to a 10 ml aliquot of 3 mg/L methylene blue solution at the optimised temperature and time. After treatment, the amount of dye remaining in solution was determined by colorimetry. Subsequently a fresh aliquot of dye solution was treated using the nanofibers from the previous test and the proportional dye removal calculated. The cycle was repeated until the proportional removal of dye was only 50%. In each cycle to evaluate reusability, the proportional desorption was also evaluated to gauge the nanofibers' uptake and thus determine their reusability. After adsorption the copolymer was re-dissolved in distilled water and the dye leaching from the polymer was studied to calculate desorption – Equation (7):

$$\%\ \text{desorption} = \frac{\text{Conc of dye leached}}{\text{Conc of dye adsorbed}} \times 100 \tag{7}$$

RESULTS AND DISCUSSION

Determination of LCST of the copolymer

The LCST values obtained from the CP measurements were confirmed using a differential scanning calorimeter. Figure 2(a) shows the thermogram for CoP-1 and Table 2 summarises the DSC events for the other copolymers. The LCSTs of the homopolymers NIPAAM and DMAEMA are 32 and 49 °C

Water Practice & Technology Vol 14 No 2
doi: 10.2166/wpt.2019.014

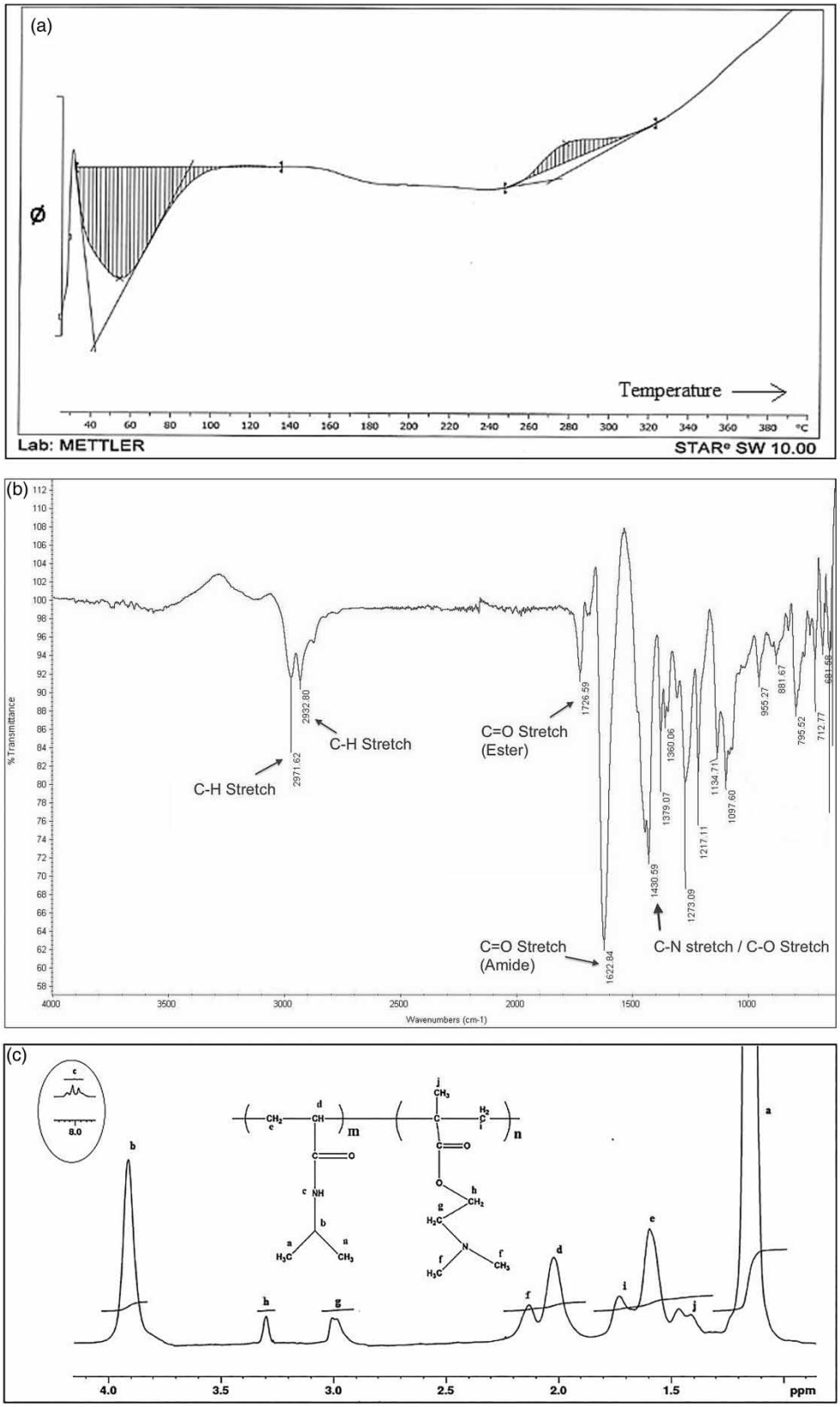

Figure 2 | (a) DSC thermogram for CoP-1 (b) FT-IR spectrum of CoP-1 (c) ^{1}H-NMR spectrum of CoP-1.

respectively. It is noted that the LCST of the copolymers differs from those of the individual homopolymers, indicating that the LCST variation is due to increase/decrease of the hydrophilic properties of the copolymer owing to addition or change of functional groups.

Water Practice & Technology Vol 14 No 2
doi: 10.2166/wpt.2019.014

Table 2 | Endothermic events by DSC and molecular weights by GPC for copolymers

	Endothermic events (°C)			Molecular weights		
Copolymer	Onset (LCST)	Peak	Endset	M_n (D)	M_w (D)	D
CoP-1	37.5	62.5	86	71,460	71,893	1.01
CoP-2	25.6	39.5	53.7	25,171	31,091	1.23
CoP-4	44.2	65.1	90	30,026	32,490	1.08

FT-IR analysis

The FT-IR spectrum of copolymer CoP-1 confirms its structure as seen in Figure 2(b). The absorption at 1,726.5 cm^{-1} is assigned to the ester C = O stretch, while the peak at 1,622.84 cm^{-1} is the amide group C = O. The presence of the ester and amide groups is reinforced by the absorption at 1,430.6 cm^{-1}, caused by the C-N and C-O stretches. The FT-IR spectra of the other copolymers reveal similar characteristics of successful copolymerization.

^{1}H-NMR Characterization

In the ^{1}H-NMR spectrum of CoP-1 (Figure 2(c)), the strong signal at 1.10 ppm is assigned to the -CH $(C\underline{H}_3)_2$ methyl from the isopropyl group in NIPAAM as is that at 3.90 ppm, while the resonance at 2.10 ppm is the methyl resonance of the $-N(C\underline{H}_3)_2$ dimethyl group in DMAEMA. The adjacent peaks at 3.00 and 3.30 ppm are from the (-N-$C\underline{H}_2$-$C\underline{H}_2$-O-) ethyl groups in DMAEMA. The signal at 1.60 ppm is attributed to the methylene group (-$C\underline{H}_2$-CH-) from the NIPAAM backbone and that at 1.72 ppm is due to the methylene (-$C\underline{H}_2$-C-) from the DMAEMA backbone. The peak at 1.4 ppm is from the methyl group ($C\underline{H}_3$-C-) in DMAEMA. The resonance at 2.00 ppm is due to the methyne (-$C\underline{H}$-CH_2) in the NIPAAM backbone. The signal at 8.00 ppm is due to the (-$N\underline{H}$-C = O) amide group in NIPAAM. The NMR spectrum thus confirms the presence of both NIPAAM and DMAEMA in the final copolymer. (The signal strengths show that NIPAAM is present in large excess over DMAEMA.)

Molecular weight determination

Gel permeation chromatography

The number average (M_n), average molecular weight (M_w) and dispersity (D) of the various thermo-responsive copolymers are given in Table 2. The uniform distribution of molecular weight in all three samples is confirmed because the D values are all close to unity.

Surface area and porosity

The surface area and porosity of CoP-1 were calculated from the adsorption isotherm obtained by measuring the amount of gas adsorbed across a wide range of relative pressures from 10 to 70 Kpa at constant temperature (liquid nitrogen 77 K) in triplicate. The amount of gas adsorbed is correlated to the total surface area of the particles including pores in the surface. The BET specific surface of CoP-1 was determined as 0.824 m^2/g, while the BJH plot shows the pore specific surface as 0.901 m^2/g. Although the copolymer has a relatively small surface area compared to conventional adsorbents – e.g., activated charcoal (3,000 m^2/g) (Dillon *et al.* 1989) – it still exhibits effective adsorbent properties due to its high specificity at LCST, when the positions of the hydrophilic and hydrophobic groups are reversed in its regular structural scaffold. The presence of hydrophobic groups on the polymers'

Water Practice & Technology Vol 14 No 2
doi: 10.2166/wpt.2019.014

(adsorbate) surface results in low/no hydrogen bonding interaction with water molecules, thereby increasing the adsorbing surface, and thus the adsorption power and selectivity.

The BJH plot indicates pore volume and radius of 0.0073 cm^3/g and 1.2 nm, respectively. The copolymer pore widths are between 2 and 10 nm, as observed in many adsorbents like zeolites. Thus the copolymers can be classified as mesoporous according to the IUPAC classification (Dąbrowski 2001). The pore width of 2.4 nm of the copolymer CoP-1 suggests that the area available for adsorption is the same as for standard adsorbents.

Copolymer particle size at CP

The particle size, measured when the polymer precipitates at the responsive temperature, is 606 nm, compared to 650 nm when measured at the responsive pH. Precipitation of the polymer as nanosize is largely responsible for the efficient dye adsorption above the CP.

SEM analysis

Figure 3 shows SEM images of the nanofibers of two copolymers,. The nanofibers are seen to be distributed randomly in the composite. The diameter of the nanofibers was calculated from the SEM images. The average diameter (AFD), determined by measuring about one hundred fibers, is between 300 and 500 nm, confirming the nanofiber structure.

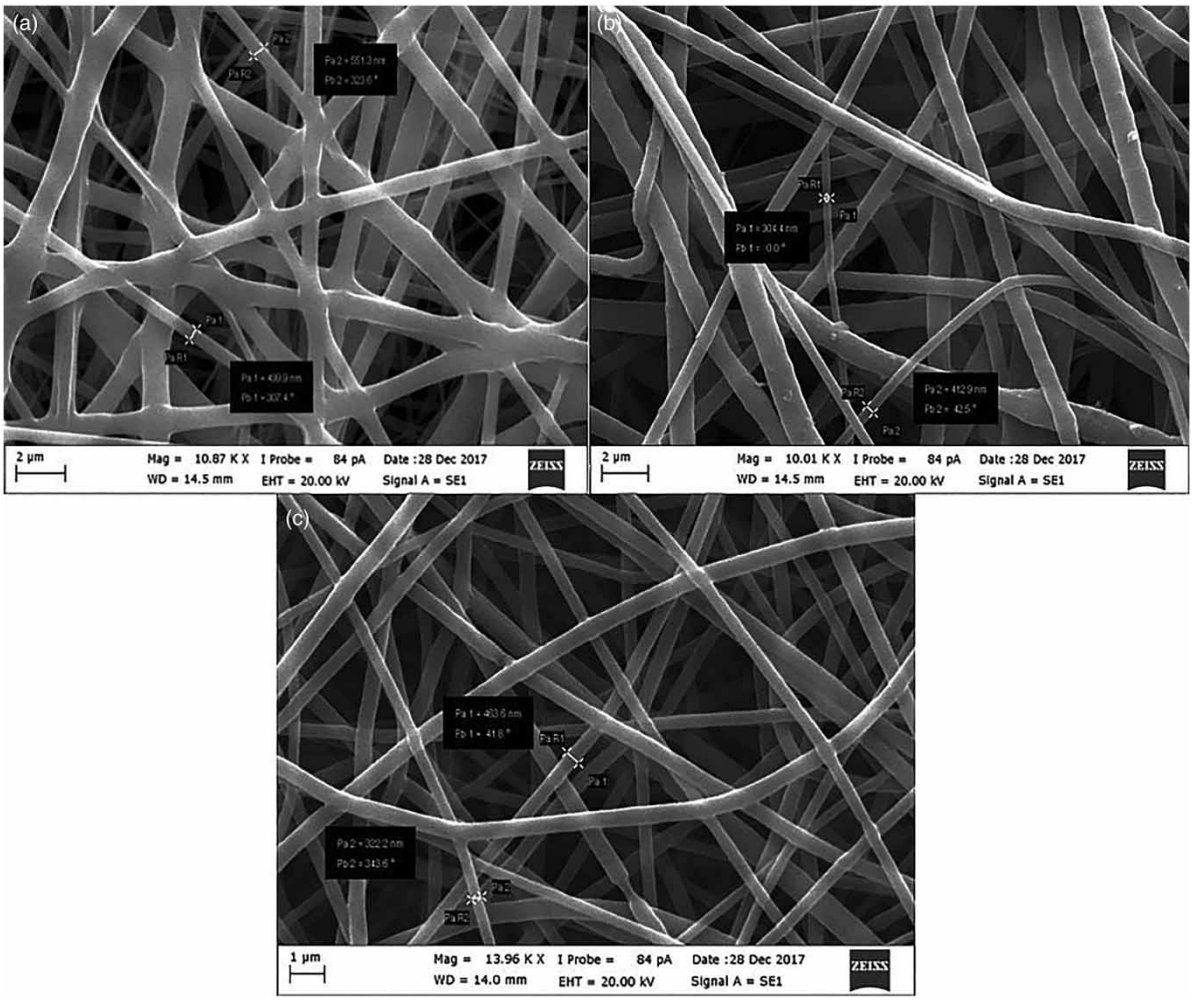

Figure 3 | SEM images for (a) NF-1 (b) NF-2 (c) PCL.

Water Practice & Technology Vol 14 No 2
doi: 10.2166/wpt.2019.014

Adsorption parameter optimization

Dual responsive polymers extract dyes effectively at the defined concentrations as shown by the decrease in absorbance with increasing contact time. Treatment continued until the solution reached equilibrium; which was attained more rapidly as the polymer concentration was increased in solution (Figure 4). The optimal copolymer concentrations and contact times were obtained for fixed dye concentrations above the respective CPs (temperature and pH) at which adsorption was studied. The optimised parameters for the copolymers treating a dye concentration of 3 mg/L are shown in Table 3.

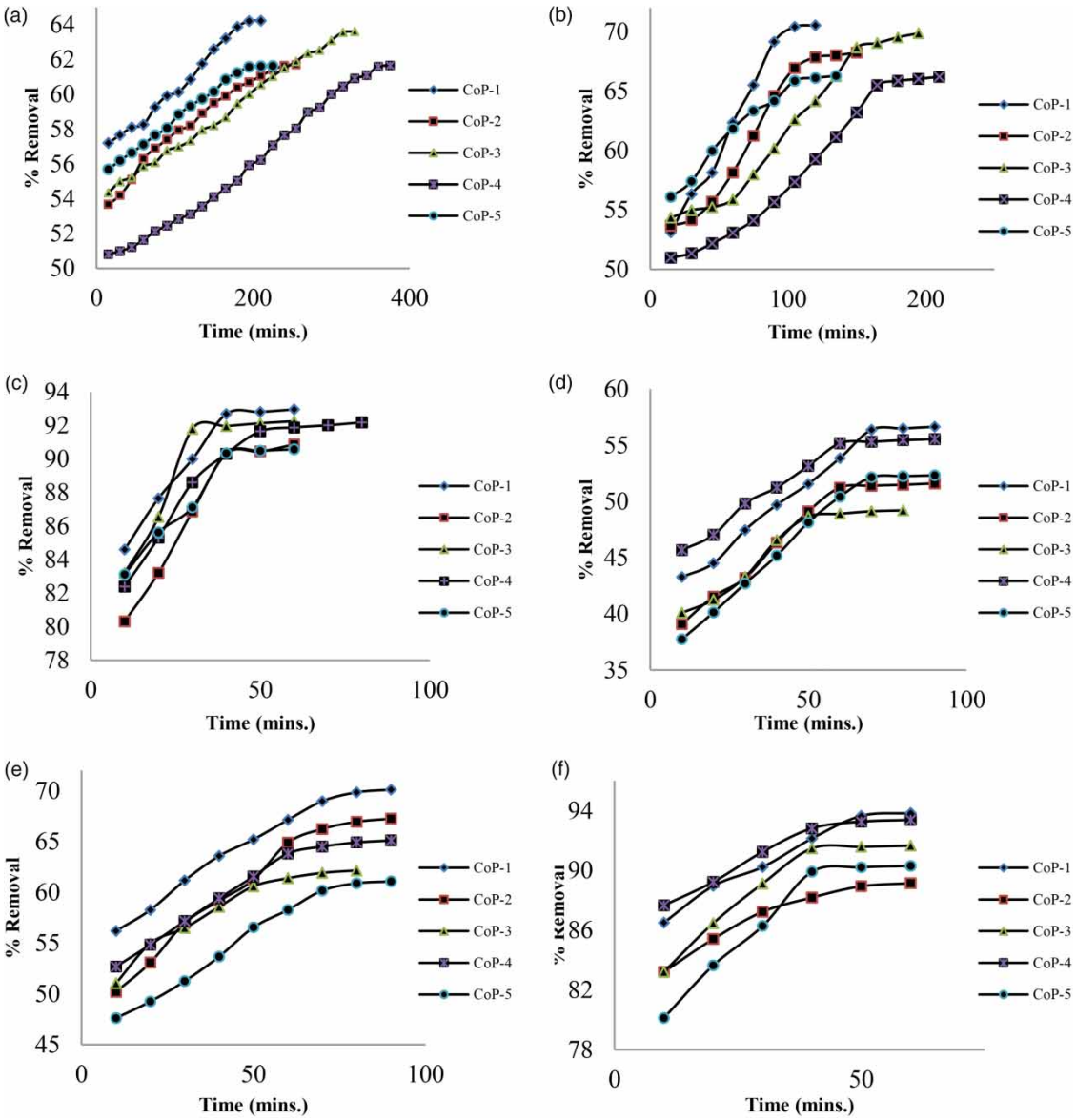

Figure 4 | Optimization of equilibrium contact time for maximum adsorption by various co-polymers at concentrations and responsive conditions as: (a) 1 mg/ml at LCST (b) 2 mg/ml at LCST (c) 4 mg/ml at LCST (d) 1 mg/ml at pH cloud point (e) 2 mg/ml at pH cloud point (f) 4 mg/ml at pH cloud point. (Values are with mean ± s.d. of 0.95–1.66).

Evaluation of adsorption potential under optimised conditions

For a polymer concentration of 4 mg/ml, the optimal temperature, pH, contact times to clear a dye (e.g. methylene blue at a concentration of 3 mg/L) was studied and the results are presented in Table 4. All of the dual responsive polymers tested exhibited similar extraction efficiencies for the

Water Practice & Technology Vol 14 No 2
doi: 10.2166/wpt.2019.014

Table 3 | Optimised conditions and maximum methylene blue removal efficiency by dual responsive polymers

	Proportional dye removal (methylene blue – 3 mg/L) (%)					
	Effect of temperature			Effect of pH		
Co-polymer (4 mg/ml)	proportional removal efficiency	Temperature	Equilibrium contact time (mins)	proportional removal efficiency	pH	Equilibrium contact time (mins)
CoP-1	92.77	40 °C	40	93.84	10.5	30
CoP-2	90.15	35 °C	40	88.26	10.5	50
CoP-3	91.32	35 °C	50	90.17	12.5	40
CoP-4	92.11	50 °C	60	93.38	11	40
CoP-5	90.49	55 °C	40	89.91	10	50

Table 4 | Proportional removal of dyes by dual responsive polymers (4 mg/ml) and nanofibers (3 mg/ml) under optimised conditions

	Proportional dye removal (%)									
	Methylene blue (3 mg/L)		Methyl orange (3 mg/L)		Indigo carmine (12 mg/L)		Congo red (20 mg/L)		Crystal violet (6 mg/L)	
Adsorbent	Temp[a]	pH[b]	Temp[a]	pH[b]	Temp[a]	pH[b]	Temp[a]	pH[b]	Temp[a]	pH[b]
CoP-1	92.77	93.84	91.26	90.97	92.60	91.24	90.28	89.86	91.20	90.41
CoP-2	90.15	88.26	89.94	89.01	90.51	89.64	88.52	87.27	90.11	88.47
CoP-3	91.32	90.17	92.16	90.43	90.57	88.63	89.74	88.02	92.20	90.18
CoP-4	92.11	93.38	90.53	89.87	91.74	90.3	90.67	89.79	90.29	89.64
CoP-5	90.49	89.91	90.12	89.16	89.65	89.12	88.2	88.47	88.95	87.88
NF-1	99.01	96.21	98.12	94.98	98.52	97.13	96.85	95.24	97.59	96.48
NF-2	97.05	95.67	95.87	94.06	96.89	95.89	95.07	93.17	95.91	96.13
NF-4	97.89	96.19	95.03	94.17	96.71	94.89	94.18	92.54	93.95	94.37
PCL Blank	54.51	53.24	49.12	51.36	53.96	51.79	56.32	55.14	50.26	49.85

[a]45 °C.
[b]12.0.

various dyes. However, CoP-1 showed maximum dye removal in the shortest contact time under the respective temperature and pH CP conditions. Since both cationic and anionic dyes were tested, this suggests that extraction is independent of the dye's charge and solely due to physical adsorption, extending the spectrum of applicability of the copolymers to a wide range of dyes.

Evaluation of adsorption potential using nanofibers

Studies were carried to determine the amount of nanofibers necessary to adsorb dye solutions of varying concentrations. This study established that 3 mg/ml nanofiber suspensions offer the maximum proportional adsorption of dye under the influence of respective trigger and contact time (Table 4). All three nanofibers – NF-1, NF-2 and NF-4 – showed slightly better dye adsorption efficiencies than the dual responsive copolymers (Table 3). PCL nanofibers also showed significant dye removal efficiency and, as the copolymers are blended with PCL for nanofabrication, the combination tends to increase their efficiency when converted to nanofibers.

Adsorption isotherm analysis

The CoP-1 and fiber NF-1 were studied using the Langmuir and Freundlich models. The models' terms were calculated and R^2 values obtained for both isotherms (Figure 5). The value of R_L shows that NF-1

Water Practice & Technology Vol 14 No 2
doi: 10.2166/wpt.2019.014

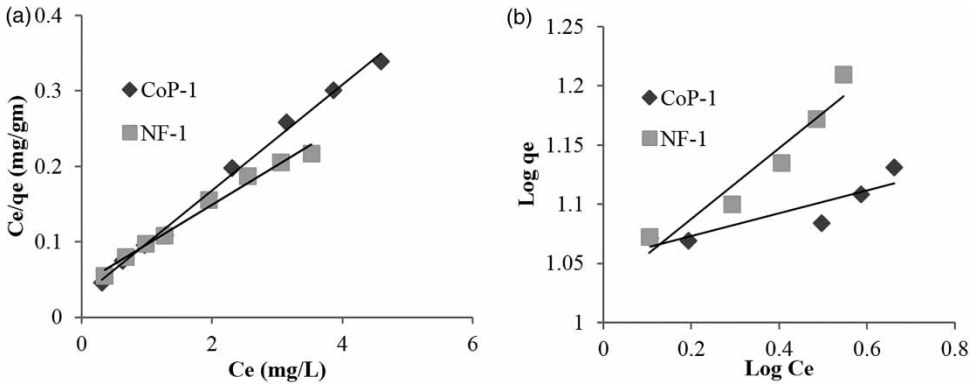

Figure 5 | Dye adsorption isotherm model onto copolymer and nanofiber substrates. (a) Langmuir and (b) Freundlich.

adsorbs the dyes better than CoP-1; in other words, converting CoP-1 to the nanofiber form NF-1 increases dye adsorption efficiency.

Table 5 shows the constants for the two isotherm models and it is evident that the Langmuir model provides a better fit than the Freundlich one for both CoP-1 ($R^2 > 0.990$) and NF-1 ($R^2 > 0.98$), indicating monolayer adsorption on the adsorbent surfaces.

Table 5 | Langmuir and Freundlich isotherm constants for dye adsorption by CoP-1 and nanofiber NF-1

	Langmuir constants				Freundlich constants		
Adsorbent	**q_m (mg/g)**	**K_L (L/mg)**	**R^2**	**R_L**	**K_F**	**1/n**	**R^2**
CoP-1	14	3.078	0.9921	0.03	0.022	0.0965	0.8034
NF-1	19	1.20	0.9856	0.076	0.012	0.2987	0.9182

Nanofiber reusability

This study was carried out at the optimised temperature, pH and time frame for maximum efficiency. As shown in Figure 6, NF-1 has slightly better dye removal efficiency of the three nanofibers tested when used repeatedly with fresh dye solution stock. All three nanofibers lose more than 50% of their efficiency after three cycles of reuse.

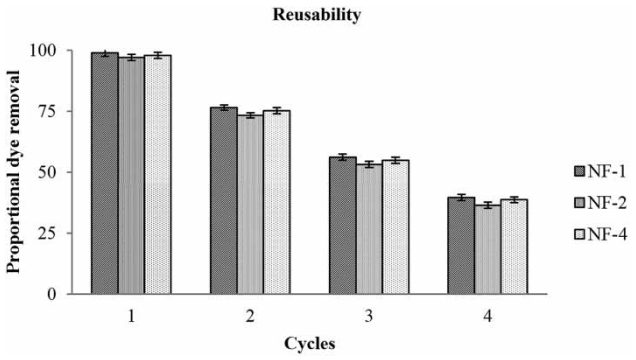

Figure 6 | Reusability of nanofibers.

CONCLUSIONS

The primary objective of the study was to develop dual responsive polymers that exhibit smart behaviour for dye removal from simulated textile water. The polymers used exhibited good adsorption

Water Practice & Technology Vol 14 No 2
doi: 10.2166/wpt.2019.014

efficiencies at various temperatures and pH levels. To improve the dye removal efficiency of the polymers, they were converted to nanofibers by electrospinning. Due to their high specific surface and sensitivity, nanofibers were found to be more effective for dye removal than polymer solutions.

ACKNOWLEDGEMENTS

The authors would like to thank: (i) University Grants Commission (UGC), India (**File No.43/489 [SR]**) for providing financial assistance for this project; (ii) SLN pharmachem and ESS-EMM for the monomer gift samples; (iii) Kingston University, London for polymer sample analysis; and (iv) Metrohm India PVT. LTD for the surface area and porosity determinations.

REFERENCES

Aguilar, M. R., Elvira, C., Gallardo, A., Vazquez, B. & Roman, J. S. 2007 Smart polymers and their applications as biomaterials. In: *Topics in Tissue Engineering*, Vol. 3. (Ashammakhi, N., Reis, R. & Chiellini, E, eds), Oulu University, Finland.

Akl, M. A. & Abou-Elanwar, A. M. 2015 Adsorption studies of cd (II) from water by acid modified multiwalled carbon nanotubes. *Journal of Nanomedicine & Nanotechnology* **6**(6), 327–336.

Chen, L., Li, Y., Hu, S., Sun, J., Du, Q., Yang, X., Ji, Q., Wang, Z., Wang, D. & Xia, Y. 2016 Removal of methylene blue from water by cellulose/graphene oxide fibress. *Journal of Experimental Nanoscience* **11**, 1156–1170.

Dąbrowski, A. 2001 Adsorption – from theory to practice. *Advances in Colloid and Interface Science* **93**, 135–224.

Dillon Jr, E. C., Wilton, J. H., Barlow, J. C. & Watson, W. A. 1989 Large surface area activated charcoal and the inhibition of aspirin absorption. *Annals of Emergency Medicine* **18**, 547–552.

Elmoubarki, R., Mahjoubi, F., Tounsadi, H., Moustadraf, J., Abdennouri, M., Zouhri, A., El Albani, A. & Barka, N. 2015 Adsorption of textile dyes on raw and decanted Moroccan clays: kinetics, equilibrium and thermodynamics. *Water Resources and Industry* **9**, 16–29.

Hinrichs, W., Schuurmans-Nieuwenbroek, N., Van De Wetering, P. & Hennink, W. 1999 Thermosensitive polymers as carriers for DNA delivery. *Journal of Controlled Release* **60**, 249–259.

Ismaya, E., Diantoro, M., Kusumaatmaja, A. & Triyana, K. 2017 Preparation of PVA/TiO_2 composites nanofibers by using electrospinning method for photocatalytic degradation. *IOP Conference Series: Materials Science and Engineering* **202**, 1–6.

Liang, C.-Z., Sun, S.-P., Li, F.-Y., Ong, Y.-K. & Chung, T.-S. 2014 Treatment of highly concentrated wastewater containing multiple synthetic dyes by a combined process of coagulation/flocculation and nanofiltration. *Journal of Membrane Science* **469**, 306–315.

Liang, M., Yang, T.-M., Chang, H.-P. & Wang, Y.-M. 2015 Dual-responsive polymer–drug nanoparticles for drug delivery. *Reactive and Functional Polymers* **86**, 27–36.

Marques, N. d. N., Maia, A. M. d. S. & Balaban, R. d. C. 2015 Development of dual-sensitive smart polymers by grafting chitosan with poly (N-isopropylacrylamide): an overview. *Polímeros* **25**, 237–246.

Paneysar, J. S., Barton, S., Chandra, S., Ambre, P. & Coutinho, E. 2017 Novel thermoresponsive assemblies of co-grafted natural and synthetic polymers for water purification. *Water Science and Technology* **75**(5), 1084–1097.

Parasuraman, D. & Serpe, M. J. 2011 Poly (N-isopropylacrylamide) microgels for organic dye removal from water. *ACS Applied Materials & Interfaces* **3**, 2732–2737.

Robinson, T., McMullan, G., Marchant, R. & Nigam, P. 2001 Remediation of dyes in textile effluent: a critical review on current treatment technologies with a proposed alternative. *Bioresource Technology* **77**, 247–255.

Samah, N. H. A. & Heard, C. M. 2013 Enhanced in vitro transdermal delivery of caffeine using a temperature-and pH-sensitive nanogel, poly (NIPAM-co-AAc). *International Journal of Pharmaceutics* **453**, 630–640.

Swaminathan, S., Muthumanickkam, A. & Imayathamizhan, N. 2015 An effective removal of methylene blue dye using polyacrylonitrile yarn waste/graphene oxide nanofibrous composite. *International Journal of Environmental Science and Technology* **12**, 3499–3508.

Zheng, Y., Wang, L., Lu, L., Wang, Q. & Benicewicz, B. C. 2017 Ph and thermal dual-responsive nanoparticles for controlled drug delivery with high loading content. *ACS Omega* **2**, 3399–3405.

Zhu, C., Jung, S., Luo, S., Meng, F., Zhu, X., Park, T. G. & Zhong, Z. 2010 Co-delivery of siRNA and paclitaxel into cancer cells by biodegradable cationic micelles based on PDMAEMA–PCL–PDMAEMA triblock copolymers. *Biomaterials* **31**, 2408–2416.